



Article

Innovative Cost-Effective Nano-NiCo₂O₄ Cathode Catalysts for Oxygen Reduction in Air-Cathode Microbial Electrochemical Systems

Qixing Zhou *, Ruixiang Li, Xiaolin Zhang and Tian Li

MOE Key Laboratory of Pollution Processes and Environmental Criteria/Tianjin Key Laboratory of Environmental Remediation and Pollution Control, College of Environmental Science and Engineering, Nankai University, Tianjin 300350, China

* Correspondence: zhouqx@nankai.edu.cn

Abstract: Microbial electrochemical systems (MESs) can harvest bioelectricity from varieties of organic matter in wastewater through electroactive microorganisms. Oxygen reduction reaction (ORR) in a cathode plays an important role in guaranteeing high power generation, which can be enhanced by cathode catalysts. Herein, the tiny crystalline grain nanocrystal NiCo₂O₄ is prepared via the economic method and utilized as an effective catalyst in air-cathode MESs. The linear sweep voltammetry results indicate that the current density of 2% nano-NiCo₂O₄/AC cathode (5.05 A/m²) at 0 V increases by 20% compared to the control (4.21 A/m²). The cyclic voltammeteries (CVs) and the electrochemical impedance spectroscopy (EIS) showed that the addition of nano-NiCo₂O₄ (2%) is efficient in boosting the redox activity. The polarization curves showed that the MESs with 2% nano-NiCo₂O₄/AC achieved the highest maximum power density (1661 ± 28 mW/m²), which was 1.11 and 1.22 times as much as that of AC and 5% nano-NiCo₂O₄. Moreover, the adulteration of nano-NiCo₂O₄ with a content of 2% can not only enable the electrical activity of the electrode to be more stable, but also reduce the cost for the same power generation in MESs. The synthetic nano-NiCo₂O₄ undoubtedly has great benefits for large-scale MESs in wastewater treatment.

Keywords: advanced green material; nano-NiCo₂O₄; wastewater treatment; oxygen reduction; green energy conversion



Citation: Zhou, Q.; Li, R.; Zhang, X.; Li, T. Innovative Cost-Effective Nano-NiCo₂O₄ Cathode Catalysts for Oxygen Reduction in Air-Cathode Microbial Electrochemical Systems. *Int. J. Environ. Res. Public Health* **2022**, *19*, 11609. <https://doi.org/10.3390/ijerph191811609>

Academic Editors: Tinggang Li and Zedong Teng

Received: 10 August 2022

Accepted: 12 September 2022

Published: 15 September 2022

Publisher's Note: MDPI stays neutral with regard to jurisdictional claims in published maps and institutional affiliations.



Copyright: © 2022 by the authors. Licensee MDPI, Basel, Switzerland. This article is an open access article distributed under the terms and conditions of the Creative Commons Attribution (CC BY) license (<https://creativecommons.org/licenses/by/4.0/>).

1. Introduction

Microbial electrochemical systems (MESs) are one of the promising green energy conversion technologies that can convert the organic substrates (e.g., organic compounds, organic waste) in wastewater into electrical energy [1]. In MESs, electroactive microorganisms (EAMs) oxidize organic substrates to generate electrons and protons, then the electrons move to the cathode through an external circuit and combine with electron acceptors [2]. Meanwhile, the protons are transported through the membrane and react with oxygen to form a water molecule [3]. In recent years, air-cathode MESs have been widely used because this configuration can gain more electrical energy from oxygen in the air as the electron acceptor without aeration [4]. However, the performance of MESs is significantly limited by poor cathode oxygen reduction reaction (ORR) and high oxygen mass transfer resistance [5]. The electrode materials play an essential role in overcoming these problems [6,7]. Therefore, the research on materials of air-cathode becomes dominant in improving the performance of MESs. Generally, carbon materials such as carbon cloth [8], carbon nanofiber [9], and active carbon (AC) [10] are used as the cathode. Among these, AC is reported to have the advantage of a large surface area (1.2 × 10⁵ m²/m² of projected surface area, 0.0026 USD/g) with higher porosity than graphite [11]. Unfortunately, the electrocatalytic activity of these cathodes made of pure carbonaceous materials is still poor when compared with other catalyst-loaded materials, and it cannot satisfy the requirement

of the four-electron pathway for high power output [12]. Therefore, it is necessary to find a material which can be doped with an activated carbon electrode to generate the similar power of MESs at a similar or lower cost.

Platinum (Pt)-based catalysts are considered the most effective catalysts in MESs because of their high ORR kinetics, but their high cost hinders their practical applications [13]. Thus, it is urgent to find low-cost and durable catalysts with high performance to replace Pt. Some of the catalysts shown in Table S1 have been reported as efficient and active, including transition metal oxides [14], non-platinum metals [15], non-metallic elements [16], and conductive polymers [17]. Among these materials, transition metal compounds have attracted attention because of their excellent catalytic activity toward the ORR. Lv et al. used broccoli-like Co-Ni₂P as an ORR catalyst with AC [18]. The maximum power density (MPD) with Co-Ni₂P/AC reached 1814 mW/m², which increased by 98% compared with the control. Ortiz-Martinez et al. used NiMn₂O₄ as catalysts, and the power output increased by 80% [19]. Compared with these transition metal oxides, NiCo₂O₄ possessed much better electrical conductivity and excellent ORR catalytic activity (Table 1). For example, Ge et al. constructed a NiCo₂O₄-modified AC air-cathode MFC. MPD of the MFC (1730 ± 14 mW/m²) was 2.28 times that of the bare AC cathode and was similar to the commercial Pt/C because of improvement to the ORR with reduced charger transfer resistance [20]. Although the addition of NiCo₂O₄ is effective in improving the power generation performance of MES, the amount of NiCo₂O₄ added in the process of fabricating electrodes has still not been thoroughly investigated, and it is unknown whether an excessive amount of NiCo₂O₄ will lead to a decrease in the economic efficiency. The cost of the cathode with 15 wt.% (45.62 mW/USD) NiCo₂O₄ is 1.2 times higher than that of the cathode with 10 wt.% NiCo₂O₄ (55.27 mW/USD). As the addition amount of NiCo₂O₄ increases, energy consumption and material costs may become negative for large-scale applications. Therefore, it is necessary to determine the ratio of NiCo₂O₄ to ensure MPD while keeping the cost as low as possible.

Table 1. The published data of the NiCo₂O₄-modified cathode.

Configuration	Application	Cathode Materials	Synthesis Methods	Power Density (mW/m ²)	Ref.
Single-chamber MFC	Power generation	Active carbon and nano urchin-like NiCo ₂ O ₄	Rolling-press	1730	[20]
Dual-chamber MFC	Power generation	Graphite plate and NiCo ₂ O ₄	Electrophoretic deposition	72	[21]
Dual-chamber MEC	Biohydrogen production	Nickel foam and NiCo ₂ O ₄ -graphene nanocomposites	Polymer binder	/	[22]
Single-chamber MFC	Power generation	Active carbon and Co ₃ O ₄ and NiCo ₂ O ₄	Rolling-press	1810	[23]
Single-chamber MFC	Power generation	Active carbon and NiCo ₂ O ₄	Hydrothermal	1676	[24]
Single-chamber MFC	Power generation	Carbon cloth and NiCo ₂ O ₄	Electrophoretic deposition	645	[25]
Dual-chamber MFC	Power generation	Acetylene black and NiCo ₂ O ₄	Hydrothermal and coating	1250	[26]

In this work, a method with the ultimate goal of economic efficiency was reported to fabricate nanocrystalline NiCo₂O₄ (<5 nm in diameter), and it was applied as a cathode catalyst in an air-cathode MES. Different concentrations (0, 2%, and 5%) of nano-NiCo₂O₄/AC composites were synthesized to optimize cathodes with the high electron transfer and ORR properties. The surface morphology and distribution of nano-NiCo₂O₄ catalysts were characterized with scanning electron microscopy (SEM) and X-ray diffraction (XRD). The catalytic performance of the synthesized cathodes was investigated by comprehensive electrochemical measurements in bioanode MESs. Finally, the production of the power density per dollar was evaluated.

2. Material and Methods

2.1. Synthesis of nano-NiCo₂O₄

NiCo₂O₄ was synthesized in three steps, as described [27]. First, 100 mg of CoCl₂•6H₂O and 61 mg of Ni(NO₃)₂•6H₂O were dissolved in 20 mL of tertiary butanol, and the solution was added to 20 mL of tertiary butanol containing 250 mg of KOH and ultrasonically dispersed for 2 h. Secondly, the resulting solution was transferred into a 50 mL autoclave and heated at 95 °C for 3 h. After that, the autoclave was cooled to room temperature. Thirdly, the obtained precipitate was centrifuged and washed with water and ethanol. Then, the precipitate was dried at 50 °C overnight. Finally, the above dry product was ground with an agate mortar. Then, the precipitate was calcined in a tube furnace at 300 °C for 3 h under an argon atmosphere, and the final product, nano-NiCo₂O₄, was obtained.

2.2. Cathode Preparation

The air-cathode, consisting of a 0.5 mm catalysis layer (CL), an electron collector (stainless steel mesh, Type 304N, 60 meshes, Detiannuo Commercial Trade Co. Ltd., Tianjin, China), and a 0.5 mm gas diffusion layer (GDL), was prepared according to the rolling-press procedure reported by our group [28]. The CL was composed of AC (Xinsen Carbon Co. Ltd., Fujian, China) and polytetrafluoroethylene (PTFE) suspension (60 wt.%, Hesen, Shanghai, China) with an AC/PTFE ratio of 6. The GDL was made by rolling a mixture of carbon black (Jinqiushi Chemical Co. Ltd., Tianjin, China) and PTFE with a mass ratio of 3:7. For the nano-NiCo₂O₄-modified cathode, different mass ratios (0, 2 wt.%, 5 wt.%) of nano-NiCo₂O₄ were added during the stirring of AC and PTFE at 80 °C in a water bath in the preparation of CL. The cathodes were named control, 2% nano-NiCo₂O₄/AC, and 5% nano-NiCo₂O₄/AC, respectively.

2.3. MES Construction and Operation

The experiments were performed on dual-chamber reactors (each cylinder chamber was 3 cm in diameter and 4 cm in length, with a net volume of 28 mL and cross-section area of 7 cm²) equipped with different NiCo₂O₄ proportioned air-cathodes [29]. All reactors were constructed by tightly bolting two cubes made of polymethyl methacrylate together. In addition, the chamber was separated by a cation exchange membrane (Ultrex CMI-7000, Membranes International Inc., Glen Rock, NJ, USA) which had been pretreated in electrolyte overnight before installment. Anodes were made of carbon fiber brushes (3 cm in diameter and 2 cm in length) pretreated with acetone and ethanol and then washed in deionized water [30].

All MESs were inoculated with the effluent from MESs operated for more than two years in our laboratory. The medium contained acetate (1.0 g/L), 50 mM phosphate buffer solution (PBS; NH₄Cl 0.31 g/L, KCl 0.13 g/L, NaH₂PO₄ 2.13 g/L, Na₂HPO₄ 4.576 g/L), trace mineral (12.5 mL/L), and vitamin solution (5 mL/L) [31]. The medium was continuously bubbled with nitrogen/carbon dioxide gas (V:V, 4:1) for 20 min to remove dissolved oxygen before filling the reactors. All solutions were refreshed when cell voltages were less than 50 mV. Reactors were operated at 25 ± 1 °C in a constant temperature incubator in the air atmosphere, and all experiments were carried out in duplicate.

2.4. Sample Characterization and Electrochemical Measurements

The topography of the sample was examined with a scanning electron microscope (SEM, Shimadzu SS-550, Japan). X-ray diffraction (XRD, D/Max2000, Rigaku, Tokyo, Japan) was used to analyze the synthesized nano-NiCo₂O₄ powder.

The voltages (V) across the 1000 Ω external resistance were recorded automatically every minute, and the average voltage was collected every 30 min using a data acquisition system (PISO-813, ICP DAS Co., Ltd., China). Cyclic voltammetry (CV) of bioanodes was performed at the scan rate of 1 mV/s over the potential from 0.2 to −0.6 V (stabilization period of 300 s). Linear sweep voltammetry (LSV) was performed in 50 mM fresh PBS at the scan rate of 0.1 mV/s (stabilization period of 300 s) over the potential from 0.3 to −0.2 V

vs. Ag/AgCl, as described previously [32]. Electrochemical impedance spectroscopy (EIS) was measured at open circuit potential (OCP) over a frequency range of 100 kHz to 0.1 Hz with a sinusoidal excitation signal of 10 mV. All CV, LSV, and EIS analyses were performed using a three-electrode system which was composed of a working electrode (WE), a counter electrode (CE, 1 cm² pt), and a Ag/AgCl (4.0 M KCl) reference electrode (RE, +198 mV vs. the standard hydrogen electrode). All electrodes were purchased from Aida Hengsheng Technology Co., Ltd., Tianjin, China, and connected to a potentiostat (Autolab PGSTAT 302N, Metrohm, Herisau, Switzerland). The difference was that the WE of CV and EIS was the bioanode, while the WE of LSV was the cathode. Polarization curves were performed with the external resistance varying from 1000 to 50 Ω in MESs as previously described [33].

3. Results and Discussion

3.1. Characterization of NiCo₂O₄ Nanoparticles and Improvement to Cathodes

The XRD technique was used to determine the phase, crystalline, and purity of the samples. The crystal structure of nano-NiCo₂O₄ was observed with XRD measurements within the range of 20°–80°, as shown in Figure 1. The main diffraction peaks could be clearly observed at 2 Theta of 31.1°, 36.7°, 44.6°, 59.1°, 65.0°, and 77.3°, corresponding to the (220), (311), (400), (511), (440), and (533) peaks, respectively, which are similar to the XRD pattern of the cubic spinel NiCo₂O₄ (JCPDS Card: 20-0781) [34,35]. Additionally, no peaks of other compounds were detectable, indicating the pure crystalline grain nanocrystal NiCo₂O₄ was successfully formed.

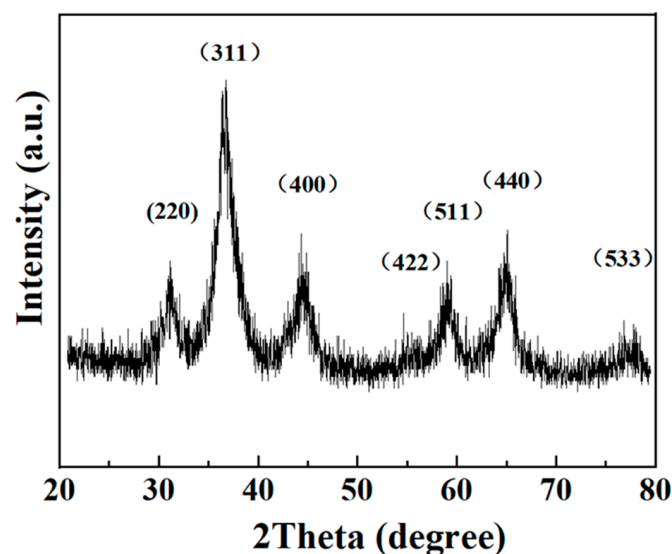


Figure 1. X-ray diffraction patterns of NiCo₂O₄.

SEM images were provided to investigate the surface morphology and the distribution of the synthesized catalysts on the electrode. Figure 2a,b show the SEM images of nanocrystal NiCo₂O₄ on the AC air-cathode. The NiCo₂O₄ nanoparticles were uniformly deposited on the surface of the cathode (Figure 2a). These nano-sized composites were reported as efficient in providing more electrochemical activity sites for oxygen access and accelerating the ORR of the electrode [36]. Figure 2c,d provide the SEM images of the AC air-cathode without NiCo₂O₄. In this cathode, AC provided more active sites for the redox reaction of NiCo₂O₄ by increasing the transport properties of ORR-relevant species [24].

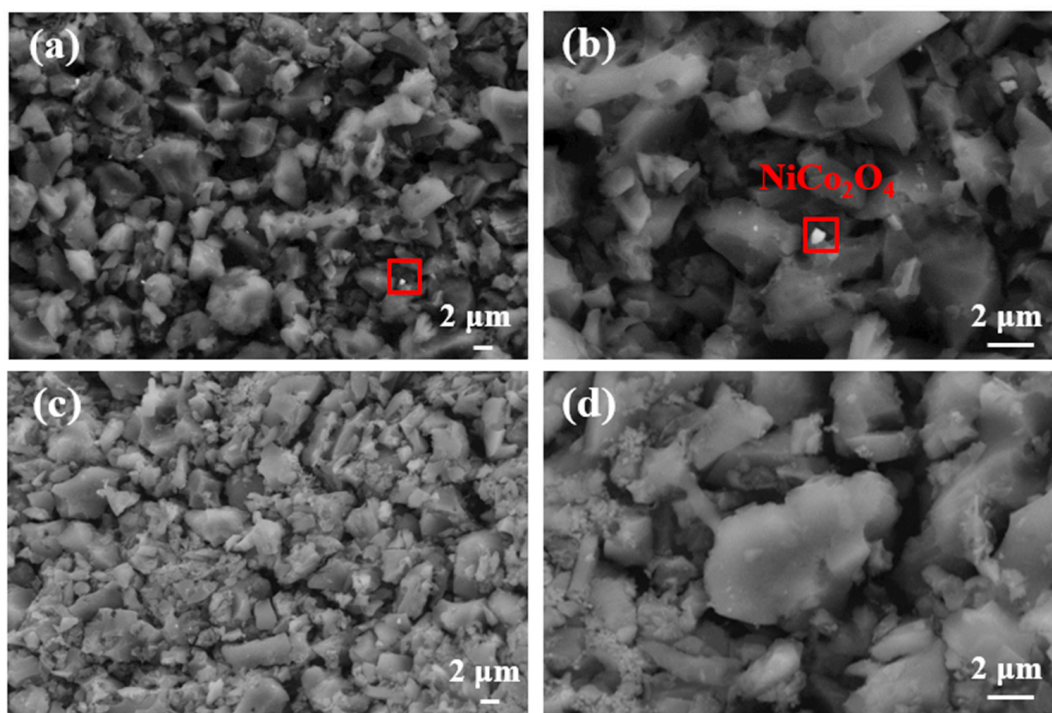


Figure 2. SEM images: (a) NiCo_2O_4 on the AC air-cathode; (b) magnified graph of the selected area in image a; (c) SEM image of bare AC air-cathode; and (d) image under the same multiple as image B of bare AC air-cathodes. The red square is considered to be the NiCo_2O_4 .

The linear sweep voltammetry curves were utilized to evaluate the electrochemical performance and ORR activity of the AC air-cathode with different proportions of NiCo_2O_4 catalysts. As shown in Figure S1, the $\text{NiCo}_2\text{O}_4/\text{AC}$ air-cathodes developed a higher current density than the control during the whole scan range. At a potential of 0 V, the current density produced by 5% $\text{NiCo}_2\text{O}_4/\text{AC}$ (5.08 A/m^2) was similar to that produced by 2% $\text{NiCo}_2\text{O}_4/\text{AC}$ (5.05 A/m^2), which showed an increase of 20% compared to the control (4.21 A/m^2). These results indicated that the NiCo_2O_4 modification promoted the ORR of the cathode. In addition, the open circuit potential (OCP) of air-cathodes was in the order of 5% $\text{NiCo}_2\text{O}_4/\text{AC}$ (0.262 V) > 2% $\text{NiCo}_2\text{O}_4/\text{AC}$ (0.249 V) > Control (0.225 V). The higher OCP indicated a higher electrochemical activity towards the ORR, indicating the effectiveness of the catalysts [23].

3.2. Power Generation Performance of MESs

The bare AC air-cathode, 2% $\text{NiCo}_2\text{O}_4/\text{AC}$ air-cathode, and 5% $\text{NiCo}_2\text{O}_4/\text{AC}$ air-cathode were used to assess the performance of power production in MESs. As presented in Figure 3, the formation of biofilm attached to the anode with the increase in voltage during 0–50 h. Although the three MESs with different cathodes did not appear to dramatically affect the time taken for power generation, the values of generated voltage are significantly different. The voltage of the MES with 2% $\text{NiCo}_2\text{O}_4/\text{AC}$ air-cathode at 50 h was 0.32 V, which was two times that of the control. After 50 h, the biofilm gradually reached maturity with the different voltage outputs. Here, the maximum voltages of AC, 2% $\text{NiCo}_2\text{O}_4/\text{AC}$, and 5% $\text{NiCo}_2\text{O}_4/\text{AC}$ were obtained in all MESs around 225 h with values of 0.57 V, 0.69 V, and 0.58 V, respectively. Compared with bare AC air-cathode MESs, the maximum voltage of the MES with 2% NiCo_2O_4 increased by 19%. The average voltages of AC, 2% $\text{NiCo}_2\text{O}_4/\text{AC}$, and 5% $\text{NiCo}_2\text{O}_4/\text{AC}$ air-cathode MESs during 5 cycles reached $0.48 \pm 0.02 \text{ V}$, $0.61 \pm 0.04 \text{ V}$, and $0.40 \pm 0.05 \text{ V}$, respectively. It could be observed that the maximum voltage and the average voltages values of AC air-cathode MESs were similar to 5% $\text{NiCo}_2\text{O}_4/\text{AC}$ air-cathode MESs and significantly lower than 2% $\text{NiCo}_2\text{O}_4/\text{AC}$

air–cathode MESs. Therefore, it was obvious that the proper introduction of transition metal oxides into AC cathodes greatly increased the maximum voltages. This phenomenon preliminarily confirmed that the NiCo_2O_4 as the cathode catalyst improved electrochemical performance and ORR activity to a certain extent compared to bare AC. Although NiCo_2O_4 had good redox activity, the conductivity of this synthesized material may be lower than AC. Thus, 5% NiCo_2O_4 in air–cathodes conversely affected the conductive performance and hindered the electron transfer process of MESs, thereby affecting the voltage output.

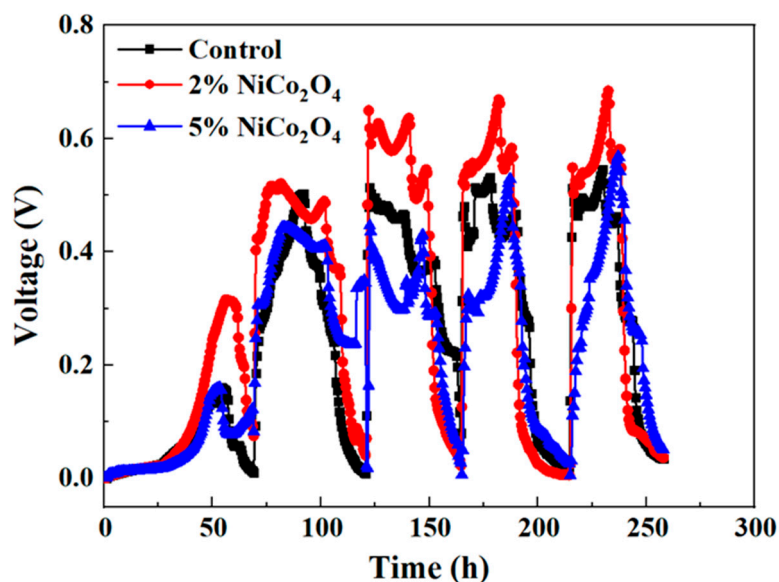


Figure 3. The output voltage of MESs with different cathodes.

3.3. Electrochemical Characterization of MESs

The cyclic voltammeteries (CVs) were performed to provide kinetic information for the heterogeneous electron-transfer reactions [37]. Here, CV analysis was carried out to investigate the performance of EAMs, which could be affected by the ORR activity of the electrodes. Sigmoidal catalytic waves and oxygen reduction peaks were observed in all CVs (Figures 4 and S2), revealing the occurrence of redox processes on the anode. Although the CVs of all the MESs with different cathodes exhibited a similar reduction peak at -0.267 ± 0.009 V, the reduction current changed with the different NiCo_2O_4 proportions. The cathode with 2% NiCo_2O_4 had a higher electroactivity towards the ORR, which could improve the performance of the bioanode. The MES with a 2% NiCo_2O_4 cathode had the highest maximum current (~ 8.54 mA), which was 1.16 and 1.30 times that of 5% NiCo_2O_4 (~ 7.34 mA) and the control (~ 6.59 mA). Moreover, at the potential of 0 V, the currents of the MESs with 2% $\text{NiCo}_2\text{O}_4/\text{AC}$, 5% $\text{NiCo}_2\text{O}_4/\text{AC}$, and control were 5.42 mA, 3.61 mA, and 4.78 mA, respectively, meaning that the proper addition of NiCo_2O_4 was efficient to boost ORR activity and thus improve the performance of MESs [38]. The addition of NiCo_2O_4 increased the activity sites for oxygen and accelerated electron transfer at the interface of electrodes [26].

To better investigate the impact of the catalyst on the charge transport of cathodes, the electrochemical impedance spectroscopy (EIS) experiments were conducted after one hour with OCP. Nyquist plots and the corresponding equivalent circuits are shown in Figure 5. The EIS was almost similarly shaped among these three MESs, with a well-defined single semicircle over the high-frequency range. There were few changes in ohmic resistance (R_s) with the value of $13.8 \pm 0.2 \Omega$ due to the use of the same reactor, fixed RE, and PBS solution in EIS tests. Differences in total resistance were mainly contributed by the charge transfer resistance (R_p). R_p usually represents the resistance of electrochemical reactions on the electrode [39]. As reported, the smaller the R_p , the faster the rate of electron transfer, which is beneficial to ORR activity [35]. R_p of 5% $\text{NiCo}_2\text{O}_4/\text{AC}$ was 4.58Ω , which was 1.7

and 1.8 times as much as that of the control (2.69 Ω), and 2% NiCo₂O₄/AC (2.55 Ω). It has been demonstrated that the smaller the charge transfer resistance (R_p), the faster the rate of electron transfer from microorganisms to the anode, which is beneficial to ORR activity, and therefore results in the improvement of current densities [35]. Therefore, the MES with a high proportion of NiCo₂O₄ (5%) could not improve the ORR activity.

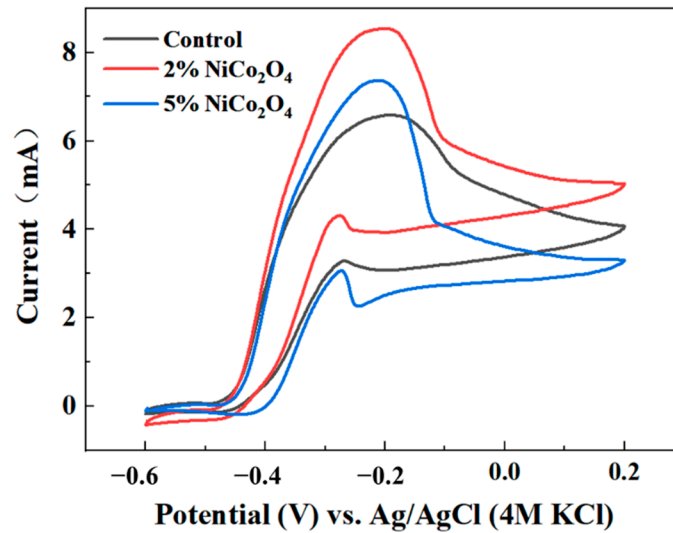


Figure 4. The cyclic voltammetry of the cathodes with 0, 2%, and 5% NiCo₂O₄ under 1 mV/s.

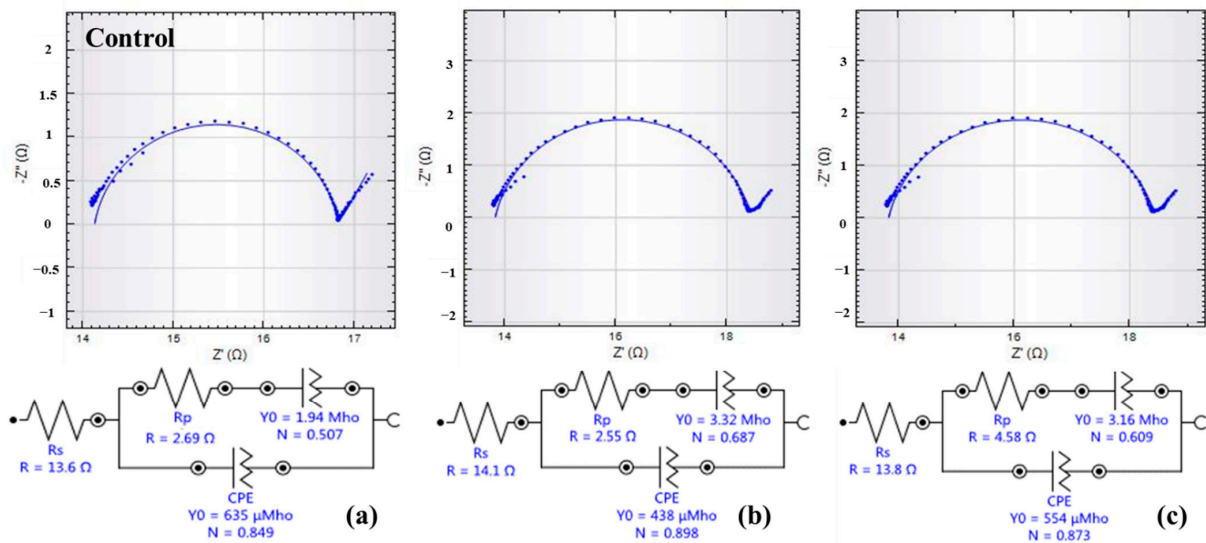


Figure 5. Nyquist plots and the equivalent circuit of the control (a), 2% NiCo₂O₄/AC (b), and 5% NiCo₂O₄/AC (c).

To further explore the electrochemical activity of the MES, the polarization curves were measured. The power density and the polarization curves for the MESs with different cathodic catalysts are illustrated in Figure 6. As shown in Figure 6a, the cathode with bare AC produced an MPD of $1499 \pm 36 \text{ mW/m}^2$, which was close to the former report [32,40], while the MES with 2% NiCo₂O₄/AC obtained the highest MPD ($1661 \pm 28 \text{ mW/m}^2$), 1.11 times as much as that of bare AC. However, the MPD of MESs with 5% NiCo₂O₄/AC was $1364 \pm 25 \text{ mW/m}^2$. The high MPD was related to both anode microbial activity and cathode catalysts with the operation of MESs. The voltage values decreased in all MESs with the increase in the current density. Therefore, the internal resistance of the MESs could be estimated by calculating the slope of the curves. From the linear fitting results, the slopes

of the different MESs in this study were almost the same (-23.50 ± 1.37) and showed a similar trend in EIS; this could be explained as the cathode with 2% NiCo₂O₄ enabled more active sites and conductive channels to electron transfer in contact with the electrolyte [26].

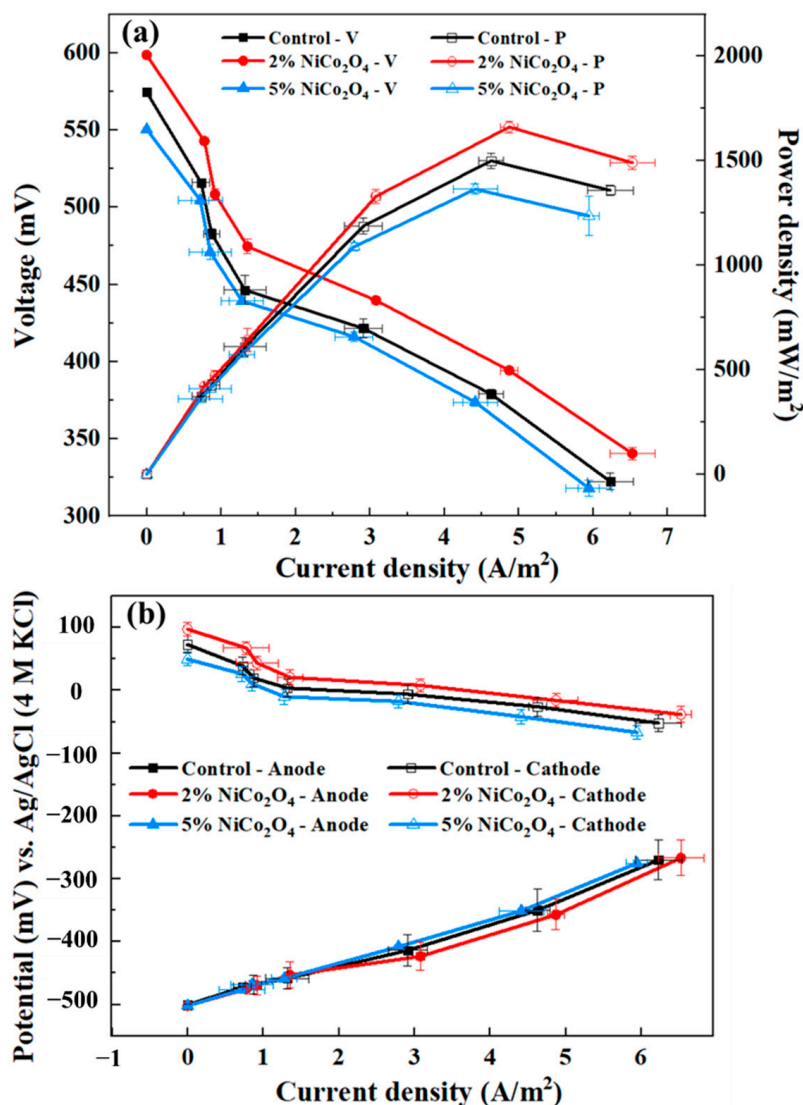


Figure 6. (a) Polarization and power density curves, and (b) individual polarization curves of cathodes and anodes during operation.

The individual polarization curve of cathodes and anodes during the operation is shown in Figure 6b. The cathode potentials of 2% NiCo₂O₄/AC were significantly higher than that of the control, indicating the 2% NiCo₂O₄/AC exhibited a better catalytic performance and ORR activities in MESs. For example, at a current density of 1.3 A/m², the cathode potential of 2% NiCo₂O₄/AC (21.89 mV) was 6.10 times that of the control (3.59 mV). In addition, the anode potentials exhibited almost the same trend, which provided further evidence that the improved performance of MESs was mainly caused by the new cathode.

4. Cost–Benefit Analysis

The low cost plays a determining factor in the application of MESs from lab-scale to large-scale, though some mid-scale MESs are operated [41]. Therefore, the cost–benefit of an MES can be improved using low-cost materials that do not significantly sacrifice performance. Due to the low cost, natural abundance, better electrochemical activity, and

higher conductivity compared with nickel and cobalt oxide, NiCo₂O₄ has been accepted as a catalyst for electrode modification. Here, the 2% nano-NiCo₂O₄/AC air-cathodes showed superior electrochemical activities and promising performance. Considering the cost of necessary chemicals and energy (October 2020), 2% nano-NiCo₂O₄ air-cathodes cost 31 USD/m², while bare ACs cost 30 USD/m² [42]. Although the total costs are similar, significant differences are found in power generated per unit cost. The cost of power generation of 2% nano-NiCo₂O₄ air-cathodes was 106.85 mW/USD, which was 1.11 times as much as that (96.31 mW/USD) of AC air-cathodes. These results indicate that a 2% nano-NiCo₂O₄/AC air-cathode could be the better alternative for large-scale applications.

5. Conclusions

The highly efficient nanocrystal NiCo₂O₄ (with a diameter lower than 5 μm) as superior ORR catalysts for air-cathode MESs were synthesized via the economic method. The MPD of the MES with the optimal modifying ratio (2%) of nano-NiCo₂O₄ was found to be 1.11 and 1.22 times as much as that of bare AC air-cathode MESs and 5% nano-NiCo₂O₄/AC MESs. The enhancement is mainly attributed to the promotion of electron transfer and reduction in activation energy for the ORR. However, the higher NiCo₂O₄ addition may hinder the availability of the terminal electron acceptor-oxygen and increase the cost. These results indicate that the new nano-NiCo₂O₄ catalyst is an affordable and easily prepared cathode catalyst. Meanwhile, the amount of nano-NiCo₂O₄ catalyst addition needs to be considered comprehensively in preparing electrodes, which is important to reduce the cost and improve the power generation of large-scale MESs.

Supplementary Materials: The following supporting information can be downloaded at: <https://www.mdpi.com/article/10.3390/ijerph191811609/s1>. References [12,15,43–52] are cited in the supplementary materials. Figure S1. The linear sweep voltammetry of the cathodes with 0, 2%, and 5% NiCo₂O₄. Figure S2. Cyclic voltammetry of the cathodes with 0, 2%, 5% NiCo₂O₄ under 10 mV/s. Table S1. The published data of different photocatalysts and their performance.

Author Contributions: Q.Z.—conceptualization, writing—original draft, writing—review and editing, visualization, validation, supervision, and project administration. R.L.—software, formal analysis, investigation, and data curation. X.Z.—methodology and writing—review and editing. T.L.—conceptualization, data curation, writing—review and editing, visualization, and project administration. All authors have read and agreed to the published version of the manuscript.

Funding: The research was financially supported by the National Key R&D Program of China (2019YFC1804104), the National Natural Science Foundation of China (U1906222), and the China Postdoctoral Science Foundation (2019M660985).

Data Availability Statement: The datasets used and analysed during the current study are available from the corresponding author upon reasonable request.

Conflicts of Interest: The authors declare no conflict of interest.

References

1. Wang, X.; Cai, Z.; Zhou, Q.; Zhang, Z.; Chen, C. Bioelectrochemical stimulation of petroleum hydrocarbon degradation in saline soil using U-tube microbial fuel cells. *Biotechnol. Bioeng.* **2012**, *109*, 426–433. [CrossRef] [PubMed]
2. Logan, B.E. Exoelectrogenic bacteria that power microbial fuel cells. *Nat. Rev. Microbiol.* **2009**, *7*, 375–381. [CrossRef] [PubMed]
3. Rabaey, K.; Verstraete, W. Microbial fuel cells: Novel biotechnology for energy generation. *Trends Biotechnol.* **2005**, *23*, 291–298. [CrossRef]
4. Wang, Z.J.; Mahadevan, G.D.; Wu, Y.C.; Zhao, F. Progress of air-breathing cathode in microbial fuel cells. *J. Power Sources* **2017**, *356*, 245–255. [CrossRef]
5. Rismani-Yazdi, H.; Carver, S.M.; Christy, A.D.; Tuovinen, I.H. Cathodic limitations in microbial fuel cells: An overview. *J. Power Sources* **2008**, *180*, 683–694. [CrossRef]
6. Zhou, M.H.; Chi, M.L.; Luo, J.M.; He, H.H.; Jin, T. An overview of electrode materials in microbial fuel cells. *J. Power Sources* **2011**, *196*, 4427–4435. [CrossRef]
7. Tang, J.; Wang, Y.; Zhao, W.; Ye, W.; Zhou, S. Porous hollow carbon tube derived from kapok fibres as efficient metal-free oxygen reduction catalysts. *Sci. China-Techol. Sci.* **2019**, *62*, 1710–1718. [CrossRef]

8. Liu, X.; Niu, Y.; Wang, L.; Guo, Q. Treatment of m-Cresol Wastewater in an Anaerobic Fluidized Bed Microbial Fuel Cell Equipped with Different Modified Carbon Cloth Cathodes. *Energy Fuels* **2020**, *34*, 10059–10066. [[CrossRef](#)]
9. Bosch-Jimenez, P.; Martinez-Crespiera, S.; Amantia, D.; Della Pirriera, M.; Forns, I.; Shechter, R.; Borrás, E. Non-precious metal doped carbon nanofiber air-cathode for Microbial Fuel Cells application: Oxygen reduction reaction characterization and long-term validation. *Electrochim. Acta* **2017**, *228*, 380–388. [[CrossRef](#)]
10. Ren, C.; Li, K.X.; Lv, C.C.; Zhao, Y.; Wang, J.J.; Guo, S. Nanorod CoFe_2O_4 modified activated carbon as an efficient electrocatalyst to improve the performance of air cathode microbial fuel cell. *J. Electroanal. Chem.* **2019**, *840*, 134–143. [[CrossRef](#)]
11. Zhang, F.; Pant, D.; Logan, B.E. Long-term performance of activated carbon air cathodes with different diffusion layer porosities in microbial fuel cells. *Biosens. Bioelectron.* **2011**, *30*, 49–55. [[CrossRef](#)]
12. Xin, S.S.; Shen, J.G.; Liu, G.C.; Chen, Q.H.; Xiao, Z.; Zhang, G.D.; Xin, Y.J. Electricity generation and microbial community of single-chamber microbial fuel cells in response to Cu_2O nanoparticles/reduced graphene oxide as cathode catalyst. *Chem. Eng. J.* **2020**, *380*, 9. [[CrossRef](#)]
13. Ben Liew, K.; Daud, W.R.W.; Ghasemi, M.; Leong, J.X.; Lim, W.S.; Ismail, M. Non-Pt catalyst as oxygen reduction reaction in microbial fuel cells: A review. *Int. J. Hydrog. Energy* **2014**, *39*, 4870–4883. [[CrossRef](#)]
14. Zhao, Y.F.; Chen, S.Q.; Sun, B.; Su, D.W.; Huang, X.D.; Liu, H.; Yan, Y.M.; Sun, K.N.; Wang, G.X. Graphene- Co_3O_4 nanocomposite as electrocatalyst with high performance for oxygen evolution reaction. *Sci Rep.* **2015**, *5*, 7. [[CrossRef](#)] [[PubMed](#)]
15. Tiwari, A.K.; Jain, S.; Mungray, A.A.; Mungray, A.K. SnO_2 :PANI modified cathode for performance enhancement of air-cathode microbial fuel cell. *J. Environ. Chem. Eng.* **2020**, *8*, 8. [[CrossRef](#)]
16. Song, Y.E.; Lee, S.; Kim, M.; Na, J.G.; Lee, J.; Kim, J.R. Metal-free cathodic catalyst with nitrogen- and phosphorus-doped ordered mesoporous carbon (NPOMC) for microbial fuel cells. *J. Power Sources* **2020**, *451*, 8. [[CrossRef](#)]
17. Papiya, F.; Pattanayak, P.; Kumar, V.; Das, S.; Kundu, P.P. Sulfonated graphene oxide and titanium dioxide coated with nanostructured polyaniline nanocomposites as an efficient cathode catalyst in microbial fuel cells. *Mater. Sci. Eng. C Mater. Biol. Appl.* **2020**, *108*, 13. [[CrossRef](#)]
18. Lv, C.; Guo, S.; Yang, T.; Li, K. Improvement of oxygen reduction capacity by activated carbon doped with broccoli-like $\text{Co-Ni}_2\text{P}$ in microbial fuel cells. *Chem. Eng. J.* **2020**, *399*, 125601. [[CrossRef](#)]
19. Ortiz-Martinez, V.M.; Touati, K.; Salar-Garcia, M.J.; Hernandez-Fernandez, F.J.; de los Rios, A.P. Mixed transition metal-manganese oxides as catalysts in MFCs for bioenergy generation from industrial wastewater. *Biochem. Eng. J.* **2019**, *151*, 9. [[CrossRef](#)]
20. Ge, B.; Li, K.; Fu, Z.; Pu, L.; Zhang, X.; Liu, Z.; Huang, K. The performance of nano urchin-like NiCo_2O_4 modified activated carbon as air cathode for microbial fuel cell. *J. Power Sources* **2016**, *303*, 325–332. [[CrossRef](#)]
21. Tajdid Khajeh, R.; Aber, S.; Zarei, M. Comparison of NiCo_2O_4 , CoNiAl-LDH , and $\text{CoNiAl-LDH@NiCo}_2\text{O}_4$ performances as ORR catalysts in MFC cathode. *Renew. Energy* **2020**, *154*, 1263–1271. [[CrossRef](#)]
22. Jayabalan, T.; Manickam, M.; Naina Mohamed, S. NiCo_2O_4 -graphene nanocomposites in sugar industry wastewater fed microbial electrolysis cell for enhanced biohydrogen production. *Renew. Energy* **2020**, *154*, 1144–1152. [[CrossRef](#)]
23. Zhang, S.; Su, W.; Li, K.X.; Liu, D.; Wang, J.J.; Tian, P. Metal organic framework-derived $\text{Co}_3\text{O}_4/\text{NiCo}_2\text{O}_4$ double-shelled nanocage modified activated carbon air-cathode for improving power generation in microbial fuel cell. *J. Power Sources* **2018**, *396*, 355–362. [[CrossRef](#)]
24. Pu, L.T.; Liu, D.; Li, K.X.; Wang, J.J.; Yang, T.T.; Ge, B.C.; Liu, Z.Q. Carbon-supported binary transition metal chalcogenide used as cathode catalyst for oxygen reduction in microbial fuel cell. *Int. J. Hydrog. Energy* **2017**, *42*, 14253–14263. [[CrossRef](#)]
25. Cao, C.; Wei, L.; Wang, G.; Shen, J. In-situ growing NiCo_2O_4 nanoplatelets on carbon cloth as binder-free catalyst air-cathode for high-performance microbial fuel cells. *Electrochim. Acta* **2017**, *231*, 609–616. [[CrossRef](#)]
26. Li, M.; Zhang, H.G.; Xiao, T.F.; Zhang, B.P.; Yan, J.; Chen, D.Y.; Chen, Y.H. Rose flower-like nitrogen-doped NiCo_2O_4 /carbon used as cathode electrocatalyst for oxygen reduction in air cathode microbial fuel cell. *Electrochim. Acta* **2017**, *258*, 1219–1227. [[CrossRef](#)]
27. Wan, L.-l.; Zang, G.-l.; Wang, X.; Zhou, L.-a.; Li, T.; Zhou, Q.-x. Tiny crystalline grain nanocrystal $\text{NiCo}_2\text{O}_4/\text{N-doped}$ graphene composite for efficient oxygen reduction reaction. *J. Power Sources* **2017**, *345*, 41–49. [[CrossRef](#)]
28. Dong, H.; Yu, H.B.; Wang, X.; Zhou, Q.X.; Feng, J.L. A novel structure of scalable air-cathode without Nafion and Pt by rolling activated carbon and PTFE as catalyst layer in microbial fuel cells. *Water Res.* **2012**, *46*, 5777–5787. [[CrossRef](#)]
29. Liao, C.M.; Wu, J.L.; Zhou, L.; Li, T.; An, J.K.; Huang, Z.L.; Li, N.; Wang, X. Repeated transfer enriches highly active electrotophic microbial consortia on biocathodes in microbial fuel cells. *Biosens. Bioelectron.* **2018**, *121*, 118–124. [[CrossRef](#)]
30. Wang, X.; Cheng, S.A.; Feng, Y.J.; Merrill, M.D.; Saito, T.; Logan, B.E. Use of Carbon Mesh Anodes and the Effect of Different Pretreatment Methods on Power Production in Microbial Fuel Cells. *Environ. Sci. Technol.* **2009**, *43*, 6870–6874. [[CrossRef](#)]
31. Li, T.; Zhou, L.A.; Qian, Y.W.; Wan, L.L.; Du, Q.; Li, N.; Wang, X. Gravity settling of planktonic bacteria to anodes enhances current production of microbial fuel cells. *Appl. Energy* **2017**, *198*, 261–266. [[CrossRef](#)]
32. Wang, X.; Feng, C.J.; Ding, N.; Zhang, Q.R.; Li, N.; Li, X.J.; Zhang, Y.Y.; Zhou, Q.X. Accelerated OH^- Transport in Activated Carbon Air Cathode by Modification of Quaternary Ammonium for Microbial Fuel Cells. *Environ. Sci. Technol.* **2014**, *48*, 4191–4198. [[CrossRef](#)] [[PubMed](#)]
33. Zhang, Y.Y.; Wang, X.; Li, X.J.; Gao, N.S.J.; Wan, L.L.; Feng, C.J.; Zhou, Q.X. A novel and high performance activated carbon air-cathode with decreased volume density and catalyst layer invasion for microbial fuel cells. *RSC Adv.* **2014**, *4*, 42577–42580. [[CrossRef](#)]

34. Huang, W.; Cao, Y.; Chen, Y.; Peng, J.; Lai, X.Y.; Tu, J.C. Fast synthesis of porous NiCo₂O₄ hollow nanospheres for a high-sensitivity non-enzymatic glucose sensor. *Appl. Surf. Sci.* **2017**, *396*, 804–811. [[CrossRef](#)]
35. Xia, W.-Y.; Tan, L.; Li, N.; Li, J.-C.; Lai, S.-H. Nickel cobaltite@nanocarbon hybrid materials as efficient cathode catalyst for oxygen reduction in microbial fuel cells. *J. Mater. Sci.* **2017**, *52*, 7539–7545. [[CrossRef](#)]
36. Watson, V.J.; Delgado, C.N.; Logan, B.E. Influence of Chemical and Physical Properties of Activated Carbon Powders on Oxygen Reduction and Microbial Fuel Cell Performance. *Environ. Sci. Technol.* **2013**, *47*, 6704–6710. [[CrossRef](#)]
37. Li, T.; Wang, X.; Zhou, Q.; Liao, C.; Zhou, L.; Wan, L.; An, J.; Du, Q.; Li, N.; Ren, Z.J. Swift Acid Rain Sensing by Synergistic Rhizospheric Bioelectrochemical Responses. *ACS Sens.* **2018**, *3*, 1424–1430. [[CrossRef](#)]
38. Huang, J.J.; Zhu, N.W.; Yang, T.T.; Zhang, T.P.; Wu, P.X.; Dang, Z. Nickel oxide and carbon nanotube composite (NiO/CNT) as a novel cathode non-precious metal catalyst in microbial fuel cells. *Biosens. Bioelectron.* **2015**, *72*, 332–339. [[CrossRef](#)]
39. Aikens, D.A. Electrochemical methods, fundamentals and applications. *J. Chem. Educ.* **2004**, *60*, 669–676.
40. Logan, B.; Cheng, S.; Watson, V.; Estadt, G. Graphite fiber brush anodes for increased power production in air-cathode microbial fuel cells. *Environ. Sci. Technol.* **2007**, *41*, 3341–3346. [[CrossRef](#)]
41. He, W.; Wallack, M.J.; Kim, K.-Y.; Zhang, X.; Yang, W.; Zhu, X.; Feng, Y.; Logan, B.E. The effect of flow modes and electrode combinations on the performance of a multiple module microbial fuel cell installed at wastewater treatment plant. *Water Res.* **2016**, *105*, 351–360. [[CrossRef](#)] [[PubMed](#)]
42. Luo, S.; He, Z. Ni-Coated Carbon Fiber as an Alternative Cathode Electrode Material to Improve Cost Efficiency of Microbial Fuel Cells. *Electrochim. Acta* **2016**, *222*, 338–346. [[CrossRef](#)]
43. Bhowmick, G.D.; Das, S.; Adhikary, K.; Ghangrekar, M.M.; Mitra, A. Using rhodium as a cathode catalyst for enhancing performance of microbial fuel cell. *Int. J. Hydrog. Energy* **2019**, *44*, 22218–22222. [[CrossRef](#)]
44. Yuan, Y.; Zhou, S.G.; Zhuang, L. Polypyrrole/carbon black composite as a novel oxygen reduction catalyst for microbial fuel cells. *J. Power Sources* **2010**, *195*, 3490–3493. [[CrossRef](#)]
45. Yuan, Y.; Ahmed, J.; Kim, S. Polyaniline/carbon black composite-supported iron phthalocyanine as an oxygen reduction catalyst for microbial fuel cells. *J. Power Sources* **2011**, *196*, 1103–1106. [[CrossRef](#)]
46. Li, M.; Zhou, S.Q. alpha-Fe₂O₃/polyaniline nanocomposites as an effective catalyst for improving the electrochemical performance of microbial fuel cell. *Chem. Eng. J.* **2018**, *339*, 539–546. [[CrossRef](#)]
47. Yang, T.; Li, K.; Pu, L.; Liu, Z.; Ge, B.; Pan, Y.; Liu, Y. Hollow-spherical Co/N-C nanoparticle as an efficient electrocatalyst used in air cathode microbial fuel cell. *Biosens. Bioelectron.* **2016**, *86*, 129–134. [[CrossRef](#)]
48. Ma, M.; You, S.; Gong, X.; Dai, Y.; Zou, J.; Fu, H. Silver/iron oxide/graphitic carbon composites as bacteriostatic catalysts for enhancing oxygen reduction in microbial fuel cells. *J. Power Sources* **2015**, *283*, 74–83. [[CrossRef](#)]
49. Noori, M.T.; Mukherjee, C.K.; Ghangrekar, M.M. Enhancing performance of microbial fuel cell by using graphene supported V₂O₅-nanorod catalytic cathode. *Electrochim. Acta* **2017**, *228*, 513–521. [[CrossRef](#)]
50. Cao, C.; Wei, L.; Su, M.; Wang, G.; Shen, J. Enhanced power generation using nano cobalt oxide anchored nitrogen-decorated reduced graphene oxide as a high-performance air-cathode electrocatalyst in biofuel cells. *RSC Adv.* **2016**, *6*, 52556–52563. [[CrossRef](#)]
51. Zhou, Q.; Ma, S.; Zhan, S. Superior photocatalytic disinfection of Ag-3D ordered mesoporous CeO₂ under visible light condition. *Appl. Catal. B Environ.* **2018**, *224*, 27–37. [[CrossRef](#)]
52. Huang, Q.S.; Zhou, P.J.; Yang, H.; Zhu, L.L.; Wu, H.Y. In situ generation of inverse spinel CoFe₂O₄ nanoparticles onto nitrogen-doped activated carbon for an effective cathode electrocatalyst of microbial fuel cells. *Chem. Eng. J.* **2017**, *325*, 466–473. [[CrossRef](#)]